

Cite this: *J. Mater. Chem.*, 2011, **21**, 3558

www.rsc.org/materials

## Dye-sensitized solar cells with TiO<sub>2</sub> nano-particles on TiO<sub>2</sub> nano-tube-grown Ti substrates†

Ho-Gyeong Yun,<sup>\*a</sup> Jong Hyeok Park,<sup>b</sup> Byeong-Soo Bae<sup>c</sup> and Man Gu Kang<sup>a</sup>

Received 3rd December 2010, Accepted 14th January 2011

DOI: 10.1039/c0jm04210b

In the present work, dye-sensitized solar cells (DSSCs) were prepared with TiO<sub>2</sub> nano-particles on TiO<sub>2</sub> nano-tube-grown Ti substrates. A slow electron recombination and a light scattering effect might have simultaneously contributed to the DSSC performance and resulted in improvements in the short-circuit current ( $J_{sc}$ ) and in the conversion efficiency.

The dye-sensitized solar cell (DSSC), which was originally developed by O'Regan and Grätzel in 1991,<sup>1</sup> is a novel photovoltaic device due to its low manufacturing cost and eco-friendly properties.<sup>2</sup> Furthermore, its certified photon-to-electron conversion efficiency recently reached 11.1%.<sup>3</sup> However, that conversion efficiency mark was established using a high-cost F/SnO<sub>2</sub> (FTO) glass substrate. A DSSC using a thin and light-weight substrate would have a greatly expanded degree of utility. Instead of conductive-layer-coated plastic films, Electronics and Telecommunications Research Institute has proposed metal substrates.<sup>4</sup> The metal foil has no temperature limitations, which makes it an excellent alternative. However, in the case of DSSCs based on metal substrates, light illumination should come from a counter electrode, *i.e.*, back illumination. Therefore, the light scattering layer,<sup>5</sup> which enhances the optical path length, should be located between 20 nm sized TiO<sub>2</sub> nano-particles (NPs) and conductive substrates. This structure causes poor adhesion of the scattering layer due to the large particle size of the scattering layer. In the meantime, vertically grown TiO<sub>2</sub> nano-tube (NT) arrays have also been studied because of the preferred reduced recombination and stronger light scattering effect.<sup>6</sup> Recently, the Grimes group has reported TiO<sub>2</sub> NT-based DSSCs with an overall conversion efficiency of 6.89%.<sup>7</sup> However, a sufficient amount of time is indispensable for the formation of a long TiO<sub>2</sub> NT array. The ability to achieve a longer TiO<sub>2</sub> NT increases with pH as long as the electrolyte remains acidic, but increasing the pH reduced the TiO<sub>2</sub> NT growth rate, and more time was required to achieve a growth–dissolution equilibrium.<sup>8</sup>

In this communication, we report the synergistic effect of a vertically grown TiO<sub>2</sub> NT and TiO<sub>2</sub> NP. Considering slow recombination and light-scattering,<sup>6</sup> TiO<sub>2</sub> NPs have been incorporated on short TiO<sub>2</sub> NT-grown Ti substrates (Fig. 1). For maximized dye uptake, a large surface area of a photoelectrode was attained by the TiO<sub>2</sub> NP, which was prepared by the well-known sol–gel method. TiO<sub>2</sub> NT-grown Ti foil performed as a substrate for the attachment of the TiO<sub>2</sub> NP. In our approach, therefore, the fabrication time and length of TiO<sub>2</sub> NT could be minimized while increasing, rather than diminishing, the surface area of the photoelectrode.

Ti foils (Goodfellow, 99.6 wt% purity) were prepared with the dimensions 15 × 15 × 0.1 mm<sup>3</sup>. Prior to electrochemical anodizing, all samples were cleaned with a mixture of acetone and alcohol. A naturally formed oxide layer at the top of the Ti foil was removed using a 0.1% HF solution under ultrasonic waves. A Ti foil was dipped into a solution of ethylene glycol containing 0.25% ammonium fluoride (NH<sub>4</sub>F) and 2% H<sub>2</sub>O and then a voltage of 50 V was applied with a platinum (Pt) counter electrode for 15–60 min.<sup>9</sup> The anodized Ti foil was cleaned with acetone and alcohol. 20 nm TiO<sub>2</sub> NPs, including paste, were coated onto the TiO<sub>2</sub> NT-formed Ti substrates using a doctor blade technique, followed by thermal treatment at 550 °C for 30 min under an air atmosphere. The prototype DSSCs were fabricated using platinum (Pt)-coated SnO<sub>2</sub> : F glass as the counter electrode. The Pt coating was carried out with the spin-coating of an H<sub>2</sub>PtCl<sub>6</sub> and ethanol solution, followed by heating at 400 °C for 30 min. Then, the DSSCs with TiO<sub>2</sub>

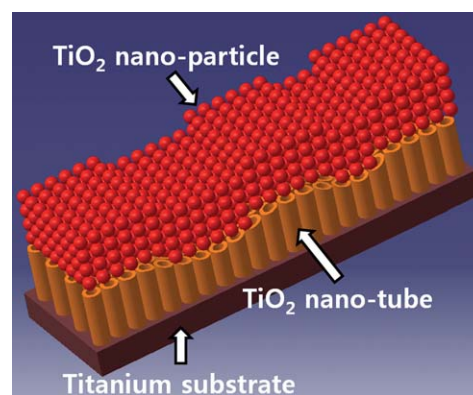


Fig. 1 Concept drawing of the photoelectrode for a DSSC composed of TiO<sub>2</sub> NP on the TiO<sub>2</sub> NT-grown Ti substrate (TiO<sub>2</sub> NP + NT/Ti).

<sup>a</sup>Convergence Components & Materials Research Laboratory, Electronics and Telecommunication Research Institute (ETRI), Daejeon, 305-350, Republic of Korea. E-mail: yunhg@etri.re.kr

<sup>b</sup>Department of Chemical Engineering, Sungkyunkwan University, Suwon, 440-746, Republic of Korea

<sup>c</sup>Laboratory of Optical Materials and Coating (LOMC), Department of Materials Science and Engineering, KAIST, Daejeon, 305-701, Korea

† Electronic supplementary information (ESI) available. See DOI: 10.1039/c0jm04210b

NP on the TiO<sub>2</sub> NT-grown Ti substrate (TiO<sub>2</sub> NP + NT/Ti) were fabricated according to the method described in our previous work.<sup>10</sup> The measured active area of the photoelectrode was approximately 0.15 cm<sup>2</sup>. The surface morphology of the Ti substrate and thickness of the TiO<sub>2</sub> layer were inspected using SEM (FEI, SIRION). The cross-sectional microstructures of the photoelectrode were characterized using scanning transmission electron microscopy (STEM) (Hitachi, HD2300A). Optical transmission was identified with UV-VIS-NIR spectrophotometers combined with an integrated sphere (Varian, Cary 100 and DRA-CA-300). Under a xenon lamp light source (Oriel, 91193), the *J*-*V* characteristics, electrochemical impedance, and voltage decay were measured using a Keithley 2400 source meter and a potentiostat/galvanostat (Gamry, Reference 600). The illumination intensity (100 mW cm<sup>-2</sup>) was adjusted with a standard solar cell composed of a crystalline Si capped with a KG-5 glass.

TiO<sub>2</sub> NT can be realized using various methods, which include electrochemical anodizing,<sup>11</sup> hydrothermal synthesis,<sup>12</sup> and template-assisted synthesis.<sup>13</sup> In particular, anodizing is a relatively simple approach for the preparation of optimized TiO<sub>2</sub> NT in terms of pore diameter, wall thickness, inter-tube spacing, and tube length.<sup>14</sup> In this experiment, anodizing of the Ti foil was used for the simple fabrication of the short TiO<sub>2</sub> NT. The total process for the preparation of the photoelectrode can be completed in 4 steps: (1) electrochemical anodizing of the Ti foil for the formation of short TiO<sub>2</sub> NT arrays, (2) doctor blading of the TiO<sub>2</sub> NP paste onto the TiO<sub>2</sub> NT-formed Ti substrates, (3) thermal treatment of the photoelectrode prepared by steps (1) and (2), and (4) dye coating of the fabricated photoelectrode.

Fig. 2(a) and (b) are the SEM images of the TiO<sub>2</sub> NP and TiO<sub>2</sub> NT. Anodizing at 50 V in a solution of ethylene glycol containing ammonium fluoride (NH<sub>4</sub>F) resulted in the formation of regular TiO<sub>2</sub> NT arrays. When the anodizing was performed for 30 min, the tube diameter and wall thickness were estimated to be about 100 and <50 nm, respectively. The lengths of the TiO<sub>2</sub> NT layers were controlled by the anodizing time. When the anodizing was performed for 15, 30, and 60 min, the lengths of the TiO<sub>2</sub> NTs were 1.53, 4.36, and 8.17 μm, respectively. After anodizing, TiO<sub>2</sub> NPs were coated onto the TiO<sub>2</sub> NT-grown Ti substrates. As shown in Fig. 2(d), TiO<sub>2</sub> NT and TiO<sub>2</sub> NP bonded well following thermal annealing at 550 °C for 30 min. It is well known that as-prepared TiO<sub>2</sub> NTs are composed of amorphous titanium oxide, but, independent of the electrolyte

composition, crystallization of the TiO<sub>2</sub> NTs to the anatase TiO<sub>2</sub> phase occurred at temperatures >280 °C.<sup>8</sup>

The TiO<sub>2</sub> NP film was made 15 μm thick, because that was the size that allowed DSSCs to exhibit optimal performance (Table 1). When the thickness of the TiO<sub>2</sub> NP was more than 15 μm, the DSSC with TiO<sub>2</sub> NP on the Ti substrate (TiO<sub>2</sub> NP/Ti) exhibited a lowered performance because the thick TiO<sub>2</sub> layer (>15 μm) provided additional electron recombination sites, resulting in a decreased open-circuit voltage (*V*<sub>oc</sub>) and fill factor (FF).<sup>15</sup> However, the DSSC with TiO<sub>2</sub> NP + NT/Ti exhibited a different behavior. Fig. 3(a) and Table 2 show the *J*-*V* characteristics of DSSCs with TiO<sub>2</sub> NP + NT/Ti compared with the DSSC with TiO<sub>2</sub> NP/Ti. As anodizing time was increased to 30 min, *i.e.* increased thickness of the TiO<sub>2</sub> NT film, the results indicated an improvement in *J*<sub>sc</sub> with a negligible effect on the *V*<sub>oc</sub> and FF. The *J*<sub>sc</sub> increased continuously with TiO<sub>2</sub> thickness<sup>16</sup> due to an increase in the number of dye molecules from the increased surface area of the TiO<sub>2</sub> film.<sup>9</sup> However, in spite of the superior surface area of the TiO<sub>2</sub> NP to TiO<sub>2</sub> NT, only the DSSC with TiO<sub>2</sub> NP + NT/Ti exhibited enhanced performance. This difference between the DSSC with TiO<sub>2</sub> NP + NT/Ti and the DSSC with TiO<sub>2</sub> NP/Ti can be attributed to the TiO<sub>2</sub> NT having an electron recombination that was reduced by comparison with the TiO<sub>2</sub> NP. The electron lifetime in the TiO<sub>2</sub> NT was longer than that in the TiO<sub>2</sub> NP because of the electron recombination suppression from the reduction in electron-hopping across the inter-crystalline contacts between the grain boundaries.<sup>16</sup>

Optical transmission is restricted to wavelengths >570 nm for a device with a TiO<sub>2</sub> layer that is more than 15 μm thick (Fig. 3(b)), resulting in a restricted increase in *J*<sub>sc</sub>. However, strong internal light scattering within the TiO<sub>2</sub> NTs elongated the path length of the long-wavelength incident light to promote the capture of photons by the dye molecules.<sup>6</sup> Despite a surface area of the DSSC with TiO<sub>2</sub> NP on 30 min anodized TiO<sub>2</sub> NT/Ti that was smaller than that of DSSC with 20 μm thick TiO<sub>2</sub> NP/Ti, the increased *J*<sub>sc</sub> could also be a result of stronger light scattering effects.

The reduced electron recombination at the interface of the TiO<sub>2</sub> NT/electrolyte was also represented in an electrochemical impedance measurement. To analyze the improved cell performance, electrochemical impedance spectra were evaluated (Fig. 3(c)). In addition, for the quantified estimation of the resistance from electrochemical impedance spectra, an equivalent circuit model including two constant phase elements has been adopted. The 1<sup>st</sup> semicircle (*R*<sub>1</sub>) occurring in the high frequency range was closely related to charge transfer at the counter electrode and/or electrical contact between the conductive substrate and TiO<sub>2</sub>.<sup>17</sup> Under the assumption that the TiO<sub>2</sub> NT is superior to TiO<sub>2</sub> NP in the interfacial contact with Ti substrates due to the *in situ* fabrication process, the largely reduced size of the 1<sup>st</sup> semicircle in a DSSC with TiO<sub>2</sub> NP + NT/Ti could be a result of the reduced electrical resistance at the interfacial contact. In the

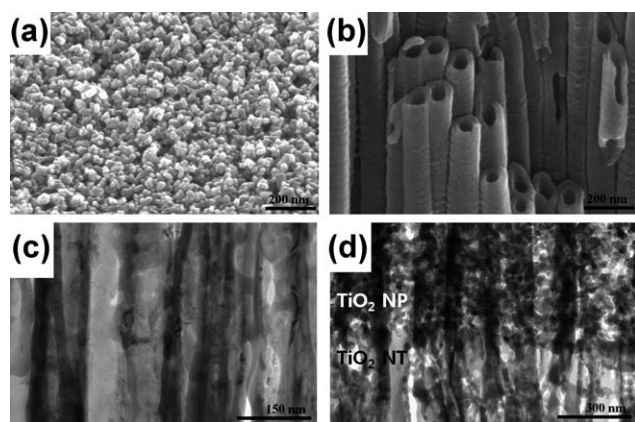


**Fig. 2** SEM images of (a) TiO<sub>2</sub> NP and (b) TiO<sub>2</sub> NT. Cross-sectional TEM images of (c) TiO<sub>2</sub> NT and (d) interface between TiO<sub>2</sub> NP and TiO<sub>2</sub> NT.

**Table 1** Summarized performance of the DSSC with TiO<sub>2</sub> NP/Ti according to the thickness of the TiO<sub>2</sub> NP layer under AM 1.5 irradiation (100 mW cm<sup>-2</sup>)

	<i>V</i> <sub>oc</sub> /V	<i>J</i> <sub>sc</sub> /mA cm <sup>-2</sup>	FF (%)	Efficiency (%)
5 μm TiO <sub>2</sub> NP	0.81	5.65	71.6	3.29
10 μm TiO <sub>2</sub> NP	0.79	7.93	69.9	4.40
15 μm TiO <sub>2</sub> NP	0.80	10.73	68.2	5.90
20 μm TiO <sub>2</sub> NP	0.73	11.49	65.9	5.54

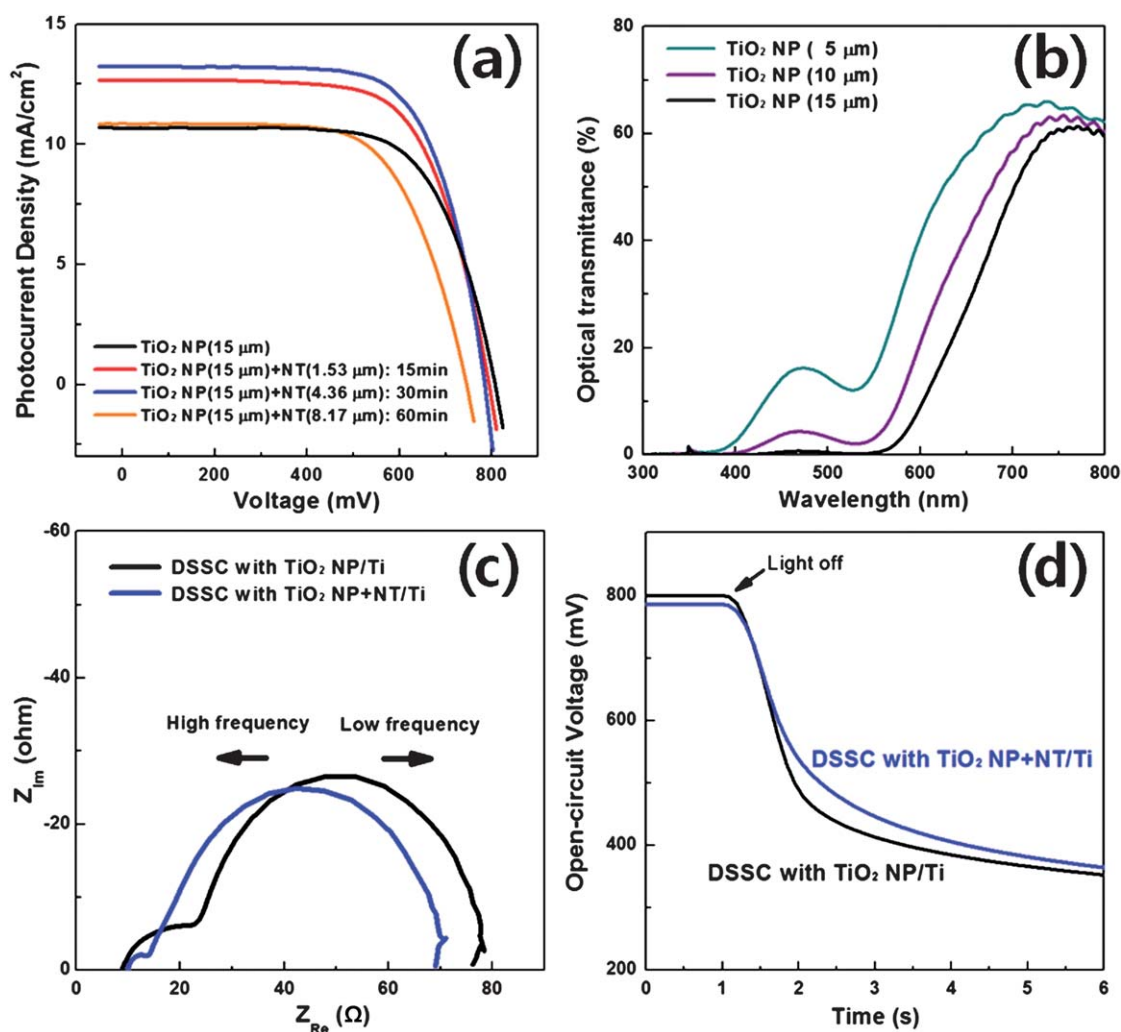


**Fig. 3** (a)  $J$ - $V$  characteristics of the DSSC with TiO<sub>2</sub> NP/Ti and TiO<sub>2</sub> NP + NT/Ti. (b) Under light from the photoelectrode direction (front illumination), optical transmission of FTO-glass-based DSSC. (c) Electrochemical impedance spectra in frequencies ranging from 10<sup>-1</sup> to 10<sup>6</sup> Hz. (d) Open-circuit voltage decay measurement.

quantified estimation, a large amount of the  $R_1$  has been varied, 16.6 Ω and 5.7 Ω in the DSSC with TiO<sub>2</sub> NP/Ti and TiO<sub>2</sub> NP + NT/Ti, respectively. However, the size of the 2<sup>nd</sup> semicircle ( $R_2$ , low frequency range) was almost the same, 53.0 Ω in the DSSC with TiO<sub>2</sub> NP/Ti and 56.0 Ω in the DSSC with TiO<sub>2</sub> NP + NT/Ti. The 2<sup>nd</sup> semicircle represents the recombination of injected electrons to the TiO<sub>2</sub> film with an electrolyte.<sup>18</sup> Under open-circuit conditions, the recombination kinetics could also be investigated by the evaluation of the rate of photovoltage decay, which is proportional to the rate of

recombination.<sup>17</sup> As shown in Fig. 3(d), DSSCs with TiO<sub>2</sub> NP/Ti and TiO<sub>2</sub> NP + NT/Ti exhibited a similar rate of photovoltage decay. The overall TiO<sub>2</sub> film in the DSSC with TiO<sub>2</sub> NP + NT/Ti was thicker than that of the DSSC with TiO<sub>2</sub> NP/Ti due to the introduction of the TiO<sub>2</sub> NT layer at the interface of the TiO<sub>2</sub> NP and Ti substrate. Therefore, it seems that the small variation in the 2<sup>nd</sup> semicircle in the electrochemical impedance spectra (Fig. 3(c)) and the rate of photovoltage decay (Fig. 3(d)) can be attributed to the slow recombination characteristics of the TiO<sub>2</sub> NT.

**Table 2** Summarized performance of the DSSCs with TiO<sub>2</sub> NP/Ti and TiO<sub>2</sub> NP + NT/Ti under AM 1.5 irradiation (100 mW cm<sup>-2</sup>)

	$V_{oc}/V$	$J_{sc}/\text{mA cm}^{-2}$	FF (%)	Efficiency (%)
Only TiO <sub>2</sub> NP (15 μm)	0.80	10.73	68.2	5.90
TiO <sub>2</sub> NP (15 μm) + TiO <sub>2</sub> NT (1.53 μm)	0.79	12.71	67.4	6.80
TiO <sub>2</sub> NP (15 μm) + TiO <sub>2</sub> NT (4.36 μm)	0.79	13.30	69.3	7.23
TiO <sub>2</sub> NP (15 μm) + TiO <sub>2</sub> NT (8.17 μm)	0.75	10.86	65.4	5.30

The DSSCs with TiO<sub>2</sub> NP + NT/Ti were prepared for the synergistic effect of vertically grown TiO<sub>2</sub> NT and TiO<sub>2</sub> NP films. The slow electron recombination at the interface of the TiO<sub>2</sub> NT/electrolyte and the light scattering effect might have simultaneously contributed to DSSC performance, and could have resulted in improvements to the  $J_{sc}$  and to the conversion efficiency with only a negligible effect on the  $V_{oc}$  and FF. Consequently, an overall conversion efficiency of 7.23% was achieved by the use of the DSSC with TiO<sub>2</sub> NP + NT/Ti.

## Acknowledgements

This work was supported by the New Renewable Energy R&D Program of the Ministry of Knowledge Economy, Republic of Korea [2009T100100528].

## Notes and references

- O'Regan and M. Grätzel, *Nature*, 1991, **353**, 737.
- M. K. Nazeeruddin, P. Pechy, T. Renouard, S. M. Zakeeruddin, B. R. Humphry, P. Comte, P. Liska, L. Cevey, E. Costa, V. Shklover, L. Spiccia, G. B. Deacon, C. A. Bignozzi and M. Grätzel, *J. Am. Chem. Soc.*, 2001, **123**, 1613.
- Y. Chiba, A. Islam, Y. Watanabe, R. Komiya, N. Koide and L. Han, *Jpn. J. Appl. Phys.*, 2006, **45**, L638.
- M. G. Kang, N.-G. Park, K. S. Ryu, S. H. Chang and K.-J. Kim, *Sol. Energy Mater. Sol. Cells*, 2006, **90**, 574.
- S. Ito, S. M. Zakeeruddin, R. H. Baker, P. Liska, R. Charvet, P. Comte, M. K. Nazeeruddin, P. Pechy, M. Takata, H. Miura, S. Uchida and M. Grätzel, *Adv. Mater.*, 2006, **18**, 1202.
- K. Zhu, N. R. Neale, A. Miedaner and A. J. Frank, *Nano Lett.*, 2007, **7**, 69.
- K. Shankar, G. K. Mor, H. E. Prakasam, S. Yoriya, M. Paulose, O. K. Varghese and C. A. Grimes, *Nanotechnology*, 2007, **18**, 065707.
- Q. Y. Cai, M. Paulose, O. K. Varghese and C. A. Grimes, *J. Mater. Res.*, 2005, **20**, 230.
- J. H. Park, T.-W. Lee and M. G. Kang, *Chem. Commun.*, 2008, 2867.
- H.-G. Yun, Y. Jun, J. Kim, B.-S. Bae and M. G. Kang, *Appl. Phys. Lett.*, 2008, **93**, 133311.
- D. Gong, C. A. Grimes, O. K. Varghese, W. C. Hu, R. S. Singh, Z. Chen and E. C. Dickey, *J. Mater. Res.*, 2001, **16**, 3331.
- T. Kasuga, M. Hiramatsu, A. Hoson, T. Sekino and K. Niihara, *Langmuir*, 1998, **14**, 3160.
- P. Hoyer, *Langmuir*, 2006, **12**, 1411.
- G. K. Mor, K. Shankar, M. Paulose, O. K. Varghese and C. A. Grimes, *Nano Lett.*, 2005, **5**, 191.
- R. Kato, A. Furube, A. V. Barzykin, H. Arakawa and M. Tachiya, *Coord. Chem. Rev.*, 2004, **248**, 1195.
- C.-J. Lin, W.-Y. Yu and S.-H. Chien, *Appl. Phys. Lett.*, 2008, **93**, 133107.
- J. H. Park, Y. Jun, H.-G. Yun, S.-Y. Lee and M. G. Kang, *J. Electrochem. Soc.*, 2008, **155**, F145.
- T. Hoshikawa, M. Yamada, R. Kikuchi and K. Eguchi, *J. Electrochem. Soc.*, 2005, **152**, E68.